運輸省港湾技術研究所

港湾技術研究所報告

REPORT OF
THE PORT AND HARBOUR RESEARCH INSTITUTE
MINISTRY OF TRANSPORT

VOL. 7 NO. 3 SEPT. 1968

NAGASE, YOKOSUKA, JAPAN

港湾技術研究所報告は第7巻第1号より年4回定期的に刊行する。ただし第1巻から第6巻および欧文編第1号から第15号までは下記のとおり不定期に刊行された。

報告の入手を希望する方は論文番号を明記して港湾技術研究所長に申し込んで下さい。

和 文 篇 (Japanese Edition)

Vol. 1. No. 1 (1963)
Vol. 2. Nos. 1～3 (1963～1964)
Vol. 3. Nos. 1～7 (1964)
Vol. 4. Nos. 1～11 (1965)
Vol. 5. Nos. 1～15 (1966)
Vol. 6. Nos. 1～8 (1967)

欧 文 篇 (English Edition)

Report Nos. 1～15 (1963～1967)

The Report of the Port and Harbour Research Institute is published quarterly, either in Japanese or in occidental languages. The title and synopsis are given both in Japanese and in occidental languages.

The report prior to the seventh volume were published in two series in Japanese and English as listed above.

The copies of the Report are distributed to the agencies interested on the basis of mutual exchange of technical publication.

Inquiries relating to the Report should be addressed to the director of the Institute specifying the numbers of papers in concern.

港湾技術研究所報告 (REPORT OF P.H.R.I.)

第7巻 第3号 (Vol. 7, No. 3), 1968年9月 (Sept. 1968)

目 次 (CONTENTS)

REPORT OF THE PORT AND
HARBOUR RESEARCH INSTITUTE
Vol. 7 No. 3 (Sept. 1968)

2. Use of Natural Radioactive Tracers for the Estimation of Sources and Direction of Sand Drift

Shoji SATO*
Isao IRIE**

Synopsis

Use of natural radioactive tracers for the estimation of sources and direction of sand drift was examined for the case of the Sendai Coast, which is the northern coast of Japan and facing the Pacific Ocean. Sand samples were taken along the Sendai Coast, washed with fresh water, dried, and sieved mechanically. Heavy minerals in these samples were separated with a liquid of tetrabromo-ethane of which specific gravity is 2.95. The content of thorium in heavy minerals separated from sand samples was analyzed on the basis of radioactive equilibrium of thorium decay chain by measuring the intensity of gamma-rays emitted from ^{212}Pb (0.239 MeV). The gamma-rays were measured with a 80-channel gamma-ray spectrometer, to which a well-type NaI scintillation detector was connected. The concentration of thorium in heavy minerals and concentration of thorium in sands including heavy minerals were calculated with the results of the gamma-ray analysis.

According to the usual sedimentary analysis and statistical analysis of predominant direction of waves, it was possible to consider that the predominant direction of sand drift along the Sendai Coast north of the Abukuma River is toward the north. The concentration of thorium in sand showed distinctly the tendency to decrease gradually in the direction of sand drift, while that in heavy minerals showed the tendency to increase in the same direction, although it had much fluctuation. Those conflicting results were discussed on the basis of the sorting process of sands by waves and it was concluded that the concentration of thorium in sands is preferable as an index for the estimation of the predominant direction of sand drift because it indicates the direction more distinctly than that in heavy minerals. Finally, sources and direction of sand drift along the Sendai Coast were discussed on the basis of the distribution of concentration of thorium in sands.

* Chief of Sand Drift Laboratory, Hydraulics Division
** Member of Sand Drift Laborary, Hydraulics Division

港湾技術研究所報告
第7巻 第3号 (1968. 9)

2. 漂砂の供給源，卓越方向の推定への天然放射性トレーサーの利用について

佐藤昭二*・入江　功**

要　旨

漂砂の供給源，卓越方向を，天然放射性トレーサー追跡により推定する方法について，仙台湾海岸を例にとって調べてみた。仙台湾海岸に沿って前浜から砂を採取し，水洗い，乾燥した後，機械的にフルイ分け，各粒径域の砂中に含まれる重鉱物を，比重 2.95 の四臭化エタンを用いて分析した。しかる後重鉱物中にトリウムと比例した量で含まれる ^{212}Pb (0.239 MeV) を，ガンマ線測定により定量し，放射平衡の観点から計算によりトリウム含有率を求めた。重鉱物中の ^{212}Pb からのガンマ線測定には，80 チャンネルのガンマ線スペクトロメータを用いた。トリウムは，重鉱物中に主として含まれているので，このようにして求めた重鉱物中のトリウム含有率から，重鉱物を分析する前の，全砂中に含まれるトリウムの含有率を計算により求めた。

底質分析，波向きの統計解析等，海岸工学上一般にとられている方法による漂砂の卓越方向の推定結果からは，仙台湾に流出する主要河川の一つである阿武隈川以北での漂砂の方向は北向きであると考えることができる。海浜砂および重鉱物中のトリウム分析結果によれば，阿武隈川がトリウムの主要供給源であり，重鉱物を含めた全砂中のトリウム含有率は，この漂砂の方向，すなわち北向きに次第に減少するが，重鉱物中のトリウム含有率は，同方向に増加していることがわかった。そこで，これらの結果を，波によるフルイ分け作用にもとづいて論じ，結局重鉱物を含めた全砂中のトリウム含有率を指標にとれば，トリウム分析が，漂砂の方向推定のための有力な手段になり得るという結論が得られた。

*　水工部　漂砂研究室長
**　水工部　漂砂研究室

CONTENTS

1. Introduction

In estimating the direction of sand drift, the following factors are usually analyzed:

(1) Accretion or erosion effects of existing structures.
(2) Shore patterns in the vicinity of headlands.
(3) Statistical analysis of wave energy.
(4) Current measurement.
(5) Sedimentary analysis.

In the sedimentary analysis, sedimentary parameters are calculated from the weight accumulation curve, concentration of heavy minerals are analyzed with heavy liquids, and some particular minerals are analyzed through mineralogical analysis. Among them, the reliable method is the mineralogical analysis, which, however, needs profound mineralogical knowledge and experience, and takes much time and labor.

Kamel[1] estimated the sources and direction of sand drift by analyzing thorium and uranium in natural sand along the California Coast.

Uranium and thorium are concentrated in plutonic rocks which usually outcrop in mountaineous area. If a river flowing through the plutonic rocks opens to the coast, the distribution of concentration of thorium and uranium in natural sand along the coast will indicate distinctly the direction in which sands discharged from the river are transported.

Study on the use of natural radioactive tracers for the estimation of sources and direction of sand drift was made in the case of the Sendai Coast where the determination of the direction of sand drift is relatively easy because of its geographical conditions.

2. Natural radioactivity

Potassium, thorium and uranium are the only naturally radioactive elements present in the earth's crust in appreciable quantities. The three major mineralogical sources of potassium in rocks and their specific gravities are shown in Table 1[2].

Table—1 Major Mineralogical Sources of Potassium in Rocks and their Specific Gravities

Rock Type	Minerals	Chemical Form	Specific Gravity
Alkali Feldspars	microcline orthoclase	$KAlSi_3O_8$	2.57
Feldspathoid Mineral	leucite	$KAlSi_2O_6$	2.47
Micas	muscovite	$K(AlSi_3O_{10})Al_2(OH, F)_2$	2.8
	biotite	$K(AlSi_3O_{10})Mg_3(OH, F)_2$	3.2

These sources of potassium are contained in both plutonic rocks and volcanic rocks. Thus, it is seen that the concentration of potassium in rocks does not depend on magmatic process through which the rocks are formed. Generally,

the concentration of potassium in rocks is directly related to the acidity of the igneous rocks: the lower acidity the rocks have, the more potassium is contained. The lower acidic rocks, namely alkaline rocks, are common on the earth's surface as well as acidic rocks.

On the other hand, thorium and uranium are highly concentrated in plutonic rocks such as diorite and granite rocks which usually outcrops in mountaneous districts. Therefore, thorium and uranium are preferable to potassium as the tracers for the estimation of sources and direction of sand drift because the sources of them supplied to the coast are restricted to the rivers flowing through the plutonic rocks. The minerals rich in thorium and uranium content found in the plutonic rocks of the Abukuma district are shown in Table 2[3].

Table—2 The Minerals Rich in Thorium and Uranium Content Found in Plutonic Rocks of the Abukuma District

Mineral	Chemical Form	Thorium	Uranium	Specific Gravity
Uranite	UO_2, UO_{2+x}	0 %	88.3%	7.5~9.7
Thorogumnite	$(Th, U)(SiO_4)_{1-x}(OH)_{4x}$	22~53%	3~31%	4.1~4.6
Zircon	$ZrSiO_4$	4.4%	4.8%	4.8~3.95
Monazite	$(Ce, Th)(P, Si)O_4$	23 %	0.4%	4.5~4.6
Xenotime	YPO_4	2.2%	3.6%	4.4~5.1
Phosphuranylite	$Ca(UO_2)_4(PO_4)_2OH_47H_2O$	0 %	63.3%	4.1
Samarskite	$(Y, U, Ca, Fe, Th)_{7-8}$	3.7%	16.6%	5.69
Fergusonite	$(Y, Er, Ce, U, Th)(Nb, Ta)O_4$	3.8%	4.4%	5.0~5.8

It is seen in tables 1 and 2 that the specific gravity of minerals rich in thorium and uranium content is larger than that of common rocks ($\simeq$2.65), while the specific gravity of minerals containing potassium is nearly equal to that of common rocks. In the present study, the sources and direction of sand drift are to be estimated on the basis of the variation of the concentration of tracers along the coast resulting from the sorting of sands by waves. The variation of the concentration of heavier tracers such as that of thorium and uranium in sands, therefore, will indicate the characteristics of sand drift distinctly because of the greater difference of specific gravity. From the above reasons, thorium and uranium were chosen for the study on the use of natural radioactive tracers for the estimation of sources and direction of sand drift.

3. Procedure of Investigation

Sand samples were taken at the mid-tide level along the Sendai Coast and at the mean low water level along the Abukuma River and the Natori River which are the main rivers openning to the coast. The sampling points of sand are shown in Fig. 1. Sand samples of about 1 kg were taken by penetrating a thin-wall-tube of 5 cm in diameter into the sand perpendicularly. Sand samples thus taken in the field were washed with fresh water to remove the salt, dried and sieved mechanically with sieve-screens of 0.08, 0.125, 0.25 and 0.71 mm meshes. The sand of each size fraction was placed in tetra-bromo-ethane of which specific gravity is 2.95, and heavy minerals settled on the bottom were used as the

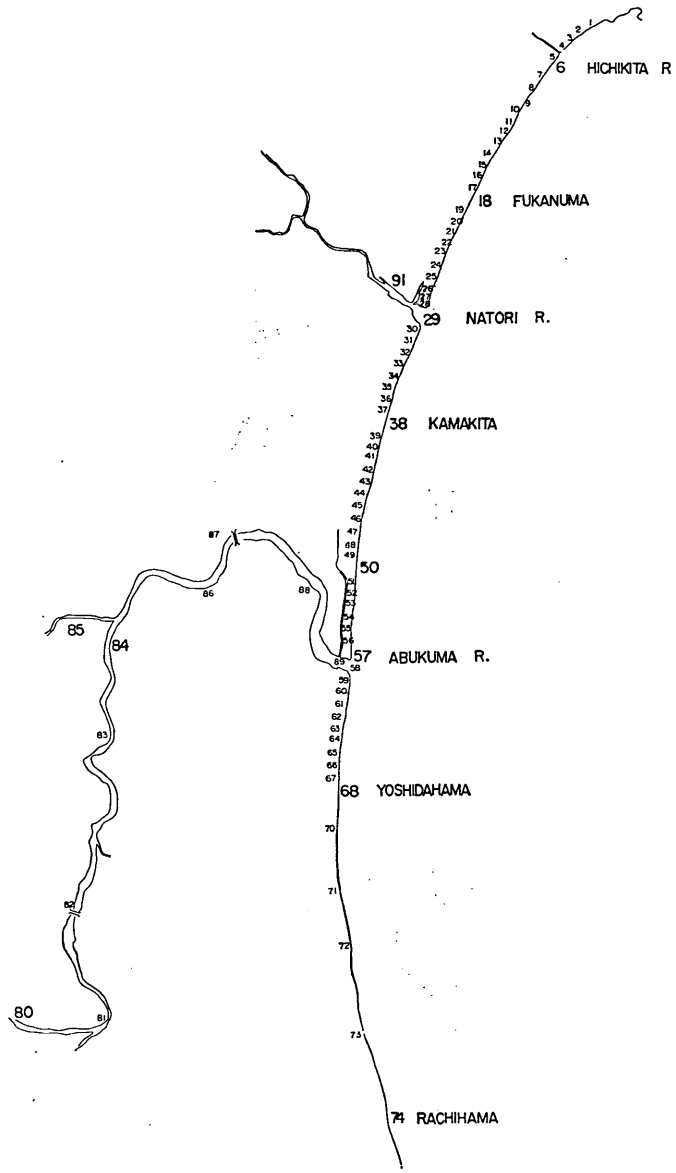

Fig. 1 Sampling Points of Sand Samples

samples for the measurement of gamma-rays because of the following reasons:

(1) Samples for the analysis of radioactivity must be concentrated so as to decrease the source absorption effect.

(2) Most of the minerals containing thorium and uranium have specific gravity larger than that of tetra-bromo-ethane; i.e. 2.95.

(3) Although potassium is an obstacle for radiological analysis of thorium and uranium, the majority of minerals containing potassium are eliminated by the separation with the heavy liquid because of their specific gravity being less than 2.95.

4. Analysis of Natural Radioactive Tracers by Means of Gamma-ray Spectrometry

1. Instrumentation

A 85 channel gamma-ray spectrometer was used for the measurement of intensity of gamma-rays emitted from the samples of heavy minerals. The radiation detector was a well-type NaI scintillation-probe as shown in Fig. 2. The sample of heavy minerals was put in a polyethylene capsule, which was then placed in the well of scintillation-probe and covered with lead shields of 10 cm in thickness in order to eliminate the background. Figure 3 shows the block-diagram of the gamma-ray spectrometer. The NaI scintillation-crystal converts the gamma radiation into the light, the intensity of which is proportional to the energy of gamma-radiation. The light pulse is converted into the electric pulse by the photo-cathode. This electric pluse is transmitted to the spectrometer and distributed

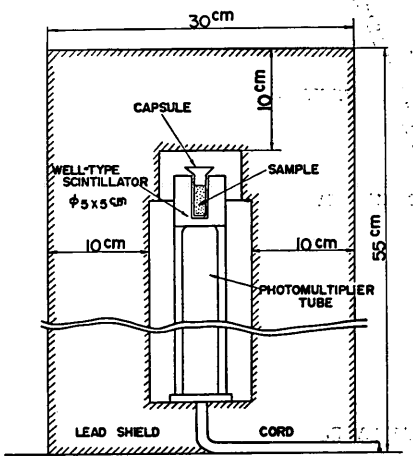

Fig. 2 Radiation Detector

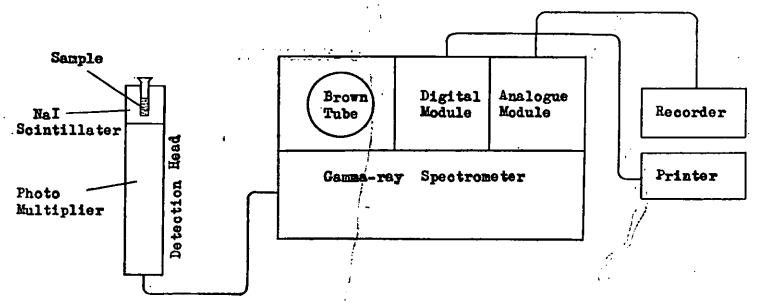

Fig. 3 Block Diagram of the Gamma-ray Spectrometer

to each channel in accordance with its energy. The energy spectrum of gamma-rays with the intensity in vertical axis and energy in horizontal axis was displayed on the Brown tube and recorded by the recorder. The figure of counting rate of gamma-rays in each channel was printed out by the digital printer.

4.2 The Nuclide Best Fitted for Measurement

A nuclide that decays to form another nuclide is called the parent, and the product is called a daughter. A decay chain is formed when the daughter decays to form another daughter, and this process are repeated one after another. In this process, the decay rate of every daughter increases and approaches to that of the parent. When the decay rate per unit time of each daughter becomes equal to the decay rate per unit time of the parent, the decay chain is in the state of radioactive equilibrium. This radioactive equilibrium can be attained

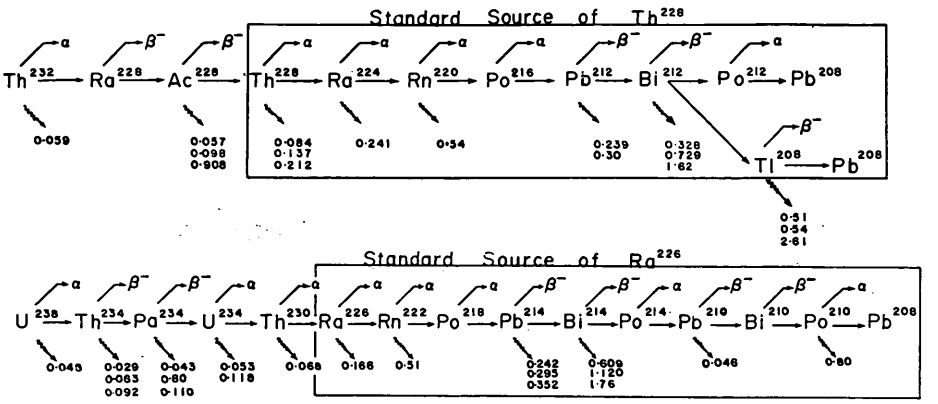

Fig. 4 Decay Chains of Thorium and Uranium

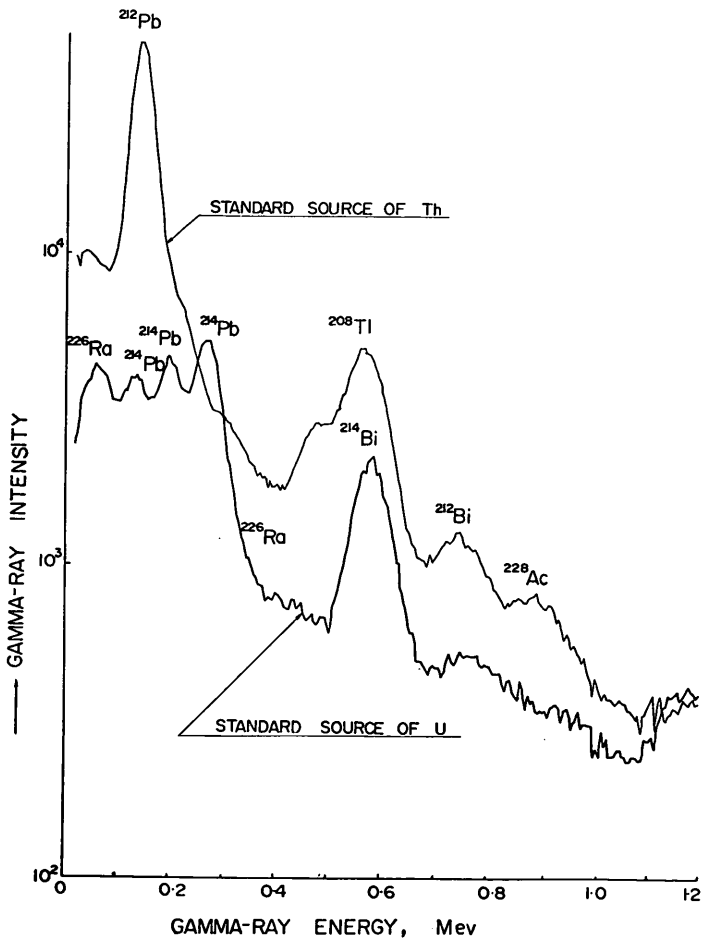

Fig. 5 Gamma-ray Spectra of Standard Sources of ^{228}Th and ^{226}Ra

after a duration nearly twice as long as the half life of the parent. Although the half lives of parents such as thorium and uranium in natural radioactivity are as long as millions of years, their decay chains must have attained radioactive equilibrium because time has passed in the same order as the half lives of thorium and uranium since magmas were frozen. Figure 4 shows the decay chains of thorium and uranium in radioactive equilibrium. Thus, the minerals which contain thorium and uranium have many nuclides which emit gamma-rays. The radioactive sources of ^{228}Th and ^{226}Ra were used in the present study as the standard sources of thorium decay chain and uranium decay chain respectively. Since these standard sources have attained radioactive equilibrium, they contain all of the nuclides following to ^{228}Th and ^{226}Ra as enclosed in Fig. 4. Figure 5 shows the gamma-ray spectra of standard sources of ^{228}Th and ^{226}Ra.

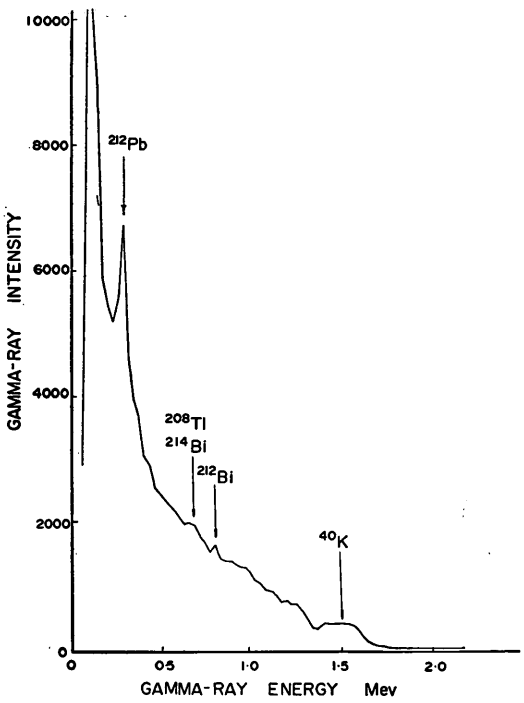

Fig. 6 An Example of Gamma-ray Spectrum of Heavy Minerals at the Mouth of the Abukuma River

When the decay chains have attained radioactive equilibrium, the measurement of gamma-ray intensity of only one daughter in each decay chain is enough for the determination of the amount of the parents, such as uranium and thorium. Adams[4] chose the high energy level of 1.86 MeV from ^{214}Bi in uranium decay chain and 2.63 MeV from ^{208}Tl in thorium decay chain. Kamel[1] chose 0.188 MeV from ^{226}Ra and 0.239 MeV from ^{212}Pb because of their high counting rate as compared with 1.86 MeV from ^{214}Bi and 2.63 MeV from ^{208}Tl. However, heavy minerals of sand taken at the Sendai Coast did not exhibit high counting rate at the energy level of 0.188 MeV. Figure 6 shows an example of gamma-ray spectrum of heavy minerals at the mouth of the Abukuma River. Only ^{212}Pb at the energy level of 0.239 MeV shows a "clean" peak and no other significant peak is seen. In the present study, therefore, only thorium was used as a tracer for the estimation of the direction of sand drift The amount of thorium in heavy minerals was calculated on the basis of radioactive equilibrium by counting the radiation of gamma-rays from ^{212}Pb.

4.3 Channel Alignment

The energy width of each channel of 80 channels is allotted at equal intervals and can be arranged with the amplification gain. Therefore, the relation between energy width and amplification gain must be given previously in order to analyze the gamma-ray intensity of a particular nuclide in gamma-ray spectrum.

This relation was obtained with three sources: ^{226}Ra (0.188 MeV), ^{228}Th (0.238 MeV) and ^{137}Cs (0.662 MeV). The result of measurement with the variation of amplification gain of horizontal axies is shown in Fig. 7. As the amplification gain

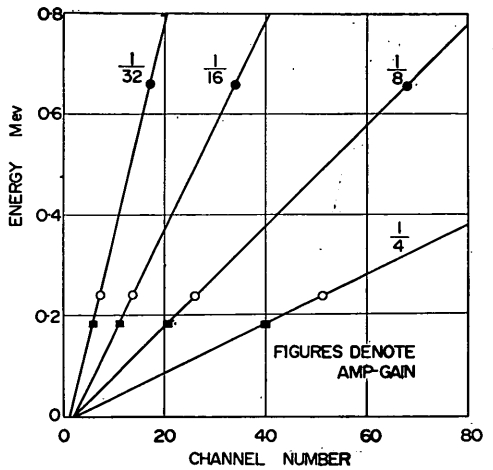

Fig. 7 Relation between Energy of Gamma-rays and Channel Number with the Variation of Horizontal Axes

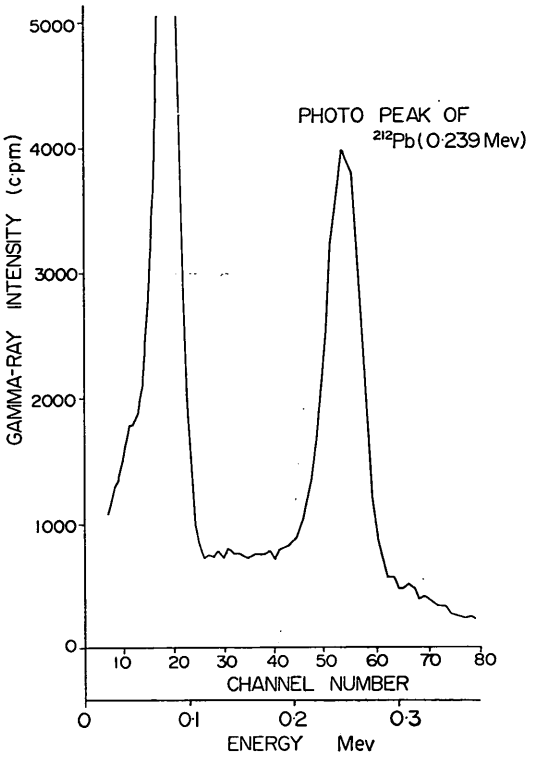

Fig. 8 Gamma-ray Spectrum of the Standard Source of ^{228}Th when the Amplification Gain is 1/4

increases, the gamma-ray spectrum is expanded horizontally and energy range of the spectrum decreases. At a given amplification gain, the gamma-ray energy is proportional to the channel number. In the present study, the energy level of 0.239 MeV of ^{212}Pb was chosen for the determination of the amount of thorium. The amplification gain was set at 1/4 so that photo-peak of ^{212}Pb is displayed at a proper position of the spectrum. The standard source used for testing the position of the photo-peak of ^{212}Pb was ^{228}Th of 3.12 Ci in activity. Figure 8 shows the gamma-ray spectrum of the standard source of ^{228}Th measured with the amplification gain decided above. The center of the photo-peak of ^{212}Pb is seen at the channel number 55. The area of this photo-peak is proportional to the amount of ^{212}Pb contained in the standard source of ^{228}Th.

4.4 Determination of detection coefficient

The counting rate of all the gamma-rays emitted from a nuclide per unit time is called the total count. No instrument is capable of measuring the total count and some leak of detection of gamma-rays is inevitable. Therefore, it is

Table—3 Details of the Standard Sources

Nuclide	Half Life	Decay Form	Gamma-rays	Intensity
Co-57	270 days	EC	0.136 Mev (10%)	0.049 Ci±10%
			0.122 (88%)	
			0.014 (6%)	
Cs-137	26.6 years		0.662 (82%)	0.047 Ci±10%
Mn-54	291 days	EC	0.842 (100%)	0.055 Ci±10%
Zn-65	245 days	EC	1,114 (44%)	0.049 Ci±10%

(Ded. 1, 1966)

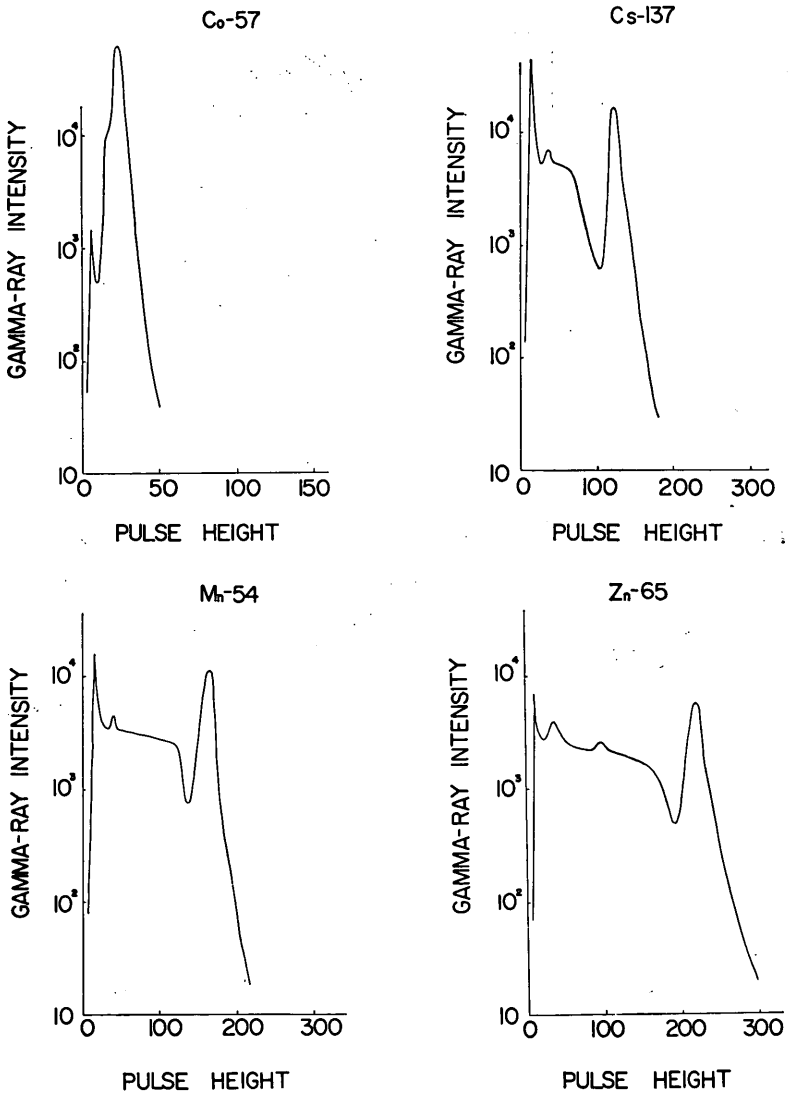

Fig. 9 Gamma-ray Spectra of Rod Type Standard Sources

very important for a quantitative analysis to know the detection coefficient, that is, the ratio of detected count to the total count. In order to determine the detection coefficient at the energy level of 0.239 MeV of ^{212}Pb, the calibrated standard source is commonly employed. Although the standard source of ^{228}Th had been calibrated accurately, the geometrical condition was not satisfied because the diameter of the capsule of the standard source was too large to insert the capsule into the well of scintillation detector shown in Fig. 2. Therefore, the detection coefficient was determined by means of interporation from the results of detection coefficient obtained by measuring several other rod type standard sources. The details of these sources are shown in Table 3, and the gamma-ray spectra of these sources are shown in Fig. 9. Since the capsules of these sources were of rod type, geometrical conditions were considered almost equivalent to that of the sample capsules. The intensity of gamma-rays of each standard source was measured and the detection coefficient for each energy level was calculated. The result of calculation is shown in Fig. 10, where the detection coefficient is seen to increase with the decrease of the energy of gamma-rays. From this figure, the detection coefficient for the energy level of 0.239 MeV of ^{212}Pb was determined to be 0.65 (65%).

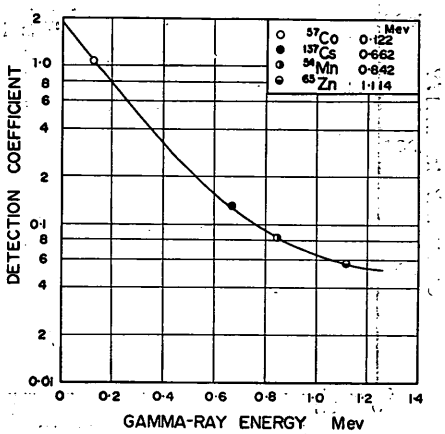

Fig. 10 Relation between Detection Coefficient and Energy of Gamma-rays

4.5 Back-Ground Consideration

It is important to eliminate the background due to cosmic-rays and radiation from the materials composing the detector, especially in the case of measuring samples of natural radioactivity of which level is as low as background. Although the detector was covered with lead shields of 10 cm in thickness, they were not enough for eliminating the background significantly.

The accuracy of radioactive counting is tested by the value of N_s^2/N_B, which is so called the figure of merit, where N_s is the count of a sample excluding background and N_B is that of background, both in the measurement period. In order to make the measurement accurate, the figure of merit must be increased as large as possible. In the low level counting, however, the count N_s of a sample cannot be increased significantly as compared with that of the background, N_B. Therefore, the ratio of N_s/N_B is difficult to be increased. The figure of merit can also be expressed:

$$N_s \times (N_s/N_B)$$

Therefore, if the total counting rate $N=N_s+N_B$ is increased, the figure of merit will increase on account of the increase of N_s. Thus, increasing the duration of measurement is the only way to make the measurement accurate when it is difficult to eliminate the background by means of instrumental device. In the present study, the duration of measurement was as long as 10 to 20 hours for one

sample. When the duration of measurement is so long, drift of energy width of each channel will cause some problem. This difficulty was overcome by running the standard source of ^{228}Th every time when the sample was exchanged.

4.6 Analysis of Gamma-Ray Spectra

Kamel calculated the content of thorium and uranium with simultaneous equation on the counting rate of the two energy levels, 0.188 MeV of ^{226}Ra and 0.238 MeV of ^{212}Pb. In the present study, since the photo-peak of ^{226}Ra did not exhibit the clean peak, amount of thorium was determined through the analysis of the area of photo-peak of ^{212}Pb at the energy level of 0.230 MeV.

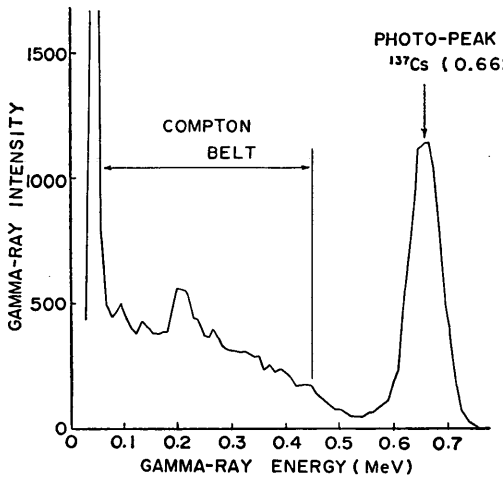

Fig. 11 Gamma-ray Spectrum of ^{137}Cs (0.662 MeV)

Figure 11 shows an example of gamma-ray spectrum of ^{137}Cs of 0.662 MeV in energy. The continuous belt from the outset of the spectrum is due to compton scattering of gamma-rays, and the peak on the right end of the spectrum is called a photo peak and the center of this peak corresponds to the energy of ^{137}Cs, namely 0.662 MeV. The area of this photo-peak is proportional to the amount of ^{137}Cs.

The heavy minerals in natural sand contain many nuclides which emit gamma-rays of various energy levels. In counting the photo-peak of ^{212}Pb of 0.239 MeV, the compton scattering due to other nuclides which have higher energy than ^{212}Pb will contribute to the counting of this photo-peak. Thus, it is complicated to analyze a particular nuclide in a sample which contains many nuclides.

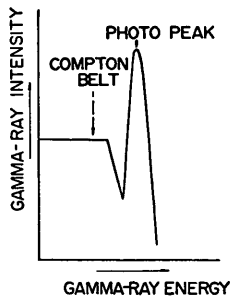

Fig. 12 Supposed Spectrum of Gamma-rays from a Nuclide

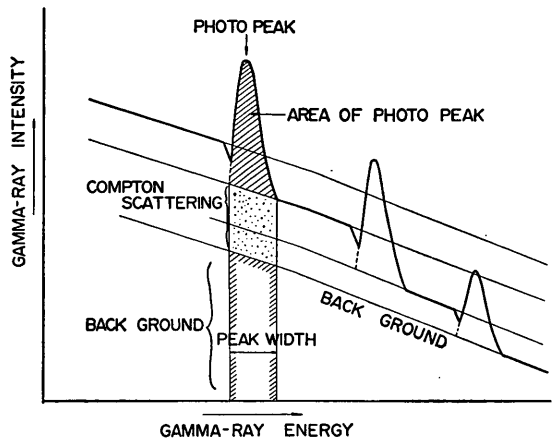

Fig. 13 Spectrum Displayed by the Gamma-ray Spectrometer

In order to simplify the analysis, the spectrum of a nuclide was supposed to have a simple distribution as shown in Fig. 12; the compton belt was supposed to be flat perfectly. Since the gamma-ray spectrum displayed by the gamma-ray spectrometer is the sum of the spectrum of sample which contains many nuclides and that of background, the spectrum will have the form as shown in Fig. 13. From this figure, the area of photo-peak of ^{212}Pb (indicated with oblique lines) is obtained by subtracting the area of the compton-belts (dotted area) and that of background from the total counting rate within the peak width. Figure 14 is an example of the analysis of gamma-ray spectrum of the heavy minerals at the mouth of the Abukuma River (Point No. 57 in Fig. 1).

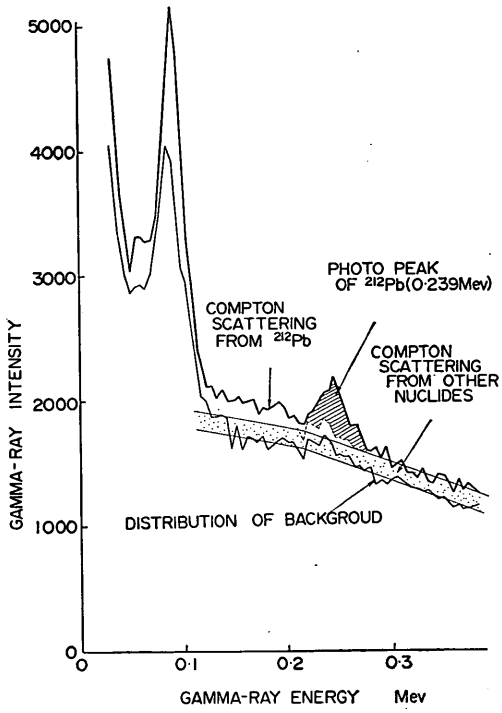

Fig. 14 An Example of the Analysis of Gamma-ray Spectrum of the Heavy Minerals at the Mouth of the Abukuma River

4.7 Calculation of Thorium Content

The content of thorium was calculated on the basis of radioactive equilibrium using the counting rate of the photo-peak of ^{212}Pb and the detection coefficient of 0.65.

In the thorium decay chain,

$$\boxed{^{232}\mathrm{Th}} \longrightarrow {}^{228}\mathrm{Ra} \longrightarrow \cdots \longrightarrow {}^{216}\mathrm{Po} \longrightarrow \boxed{^{212}\mathrm{Pb}} \longrightarrow {}^{212}\mathrm{Bi} \longrightarrow \cdots$$

if we give;

N_1=Number of atoms of ^{232}Th

T_1=Half life of ^{232}Th $\quad (1.39\times10^{10}$ years)

N_2=Number of atoms of ^{212}Pb

T_2=Half life of ^{212}Pb $\quad$ (10.6 hours)

then

$$\frac{N_1}{T_1}=\frac{N_2}{T_2} \tag{1}$$

Therefore,

$$N_2=\frac{T_2}{T_1}\cdot N_1=\frac{10.64\ \mathrm{hr}}{1.39\times10^{10}\times365\times24\ \mathrm{hr}}\times N_1$$
$$=0.874\times10^{-13}\cdot N_1 \tag{2}$$

If we assume that G p.p.m. (part per million) of ^{232}Th is contained in the heavy minerals W gr. in weight, then

$$\text{Weight of } ^{232}\text{Th} = W \cdot G \times 10^{-6} \text{ gr}$$

$$\text{Number of atoms of } ^{232}\text{Th} = \frac{232}{W \cdot G} \times 10^{-6} \times 6.02 \times 10^{23}$$

$$= 2.6 \times 10^{15} W \cdot G$$

Since this number of atoms of ^{232}Th is equal to N_1 in the equation (2),

$$N_2 = 0.874 \times 10^{-13} N_1 = 0.874 \times 10^{-13} \times (2.6 \times 10^{15} \cdot W \cdot G)$$

$$= 2.27 \times 10^{2} \cdot W \cdot G \qquad (3)$$

The decay rate C_D of ^{212}Pb is the product of decay constant $\lambda_2 \left(=\frac{0.692}{T_2}\right)$ and the number of atoms N_2 of ^{212}Pb.

Therefore, using N_2 in Fig. 3,

$$C_D = \lambda_2 N_2 = \frac{0.693}{10.64 \text{ hr}} \times 2.27 \times 10^{2} W \cdot G$$

$$= 14.8 WG \text{ (decay rate per unit hour)} \qquad (4)$$

The detection coefficient is the ratio of the counting rate C of photo-peak of ^{212}Pb to the decay rate C_D of ^{212}Pb in sample, and in the present study, this is equal to 0.65;

$$C/C_D = 0.65 \qquad (5)$$

From Eqs. (4) and (5), the content of thorium in heavy minerals G p.p.m. is shown as follows;

$$G \text{ p.p.m.} \fallingdotseq 1/10 \times (C/W) \qquad (6)$$

Therefore, if the counting rate C per unit hour of photo-peak and the weight W in grams of a sample of heavy minerals is given, the content of thorium can be calculated with the simple formula of Eq. (6).

5. Results of Analysis and Consideration

5.1 The Predominant Direction of Sand Drift Along the Sendai Coast

Sedimentary parameters such as median diameter, sorting coefficient and skewness, and the concentration of heavy minerals in sand are some indices indicating the predominant direction of sand drift. The sedimentary parameters and concentration of heavy minerals of sand samples used for the analysis of thorium were calculated for the interpretation of the predominant direction of sand drift along the Sendai Coast. Figures 15—(a) and (b) show the results of calculation and details of these are listed in Tables 4, 5. In Fig. 15—(a), the median diameter of sands is maximum at the mouths of both the Abukuma River and the Natori River and decreases gradually to the north but decreases abruptly to the south. Although the skewness and the sorting coefficient in Fig. 15—(a)

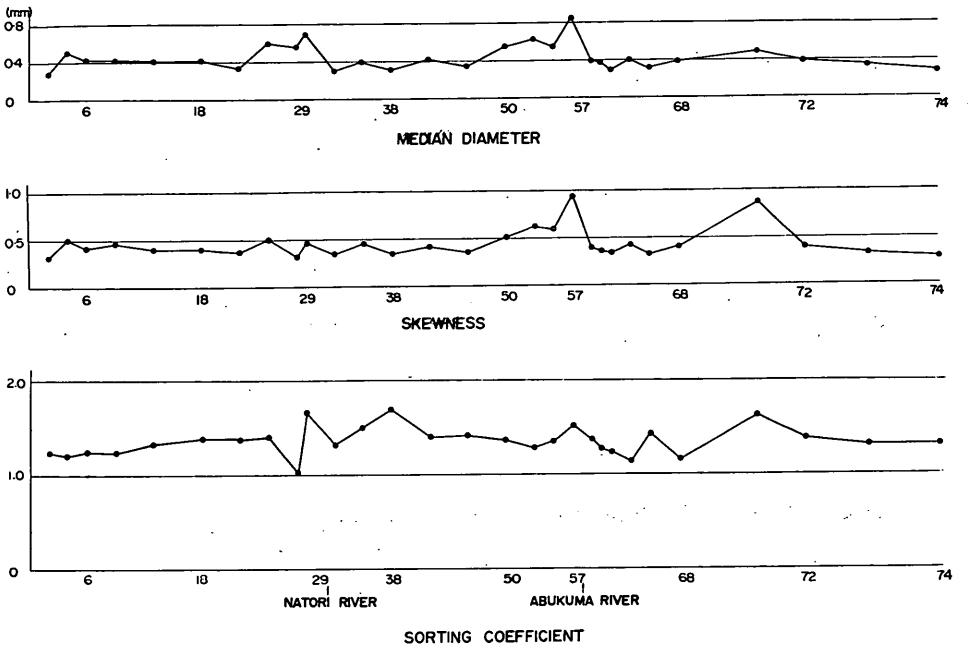

Fig. 15—(a) Distribution of Sedimentary Parameters along the Sendai Coast

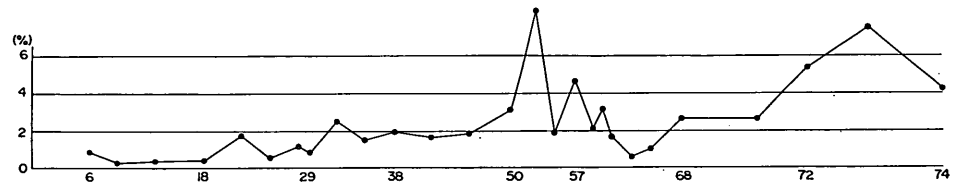

Fig. 15—(b) Distribution of the Concentration of Heavy Minerals at the Mouth of the Abukuma River

do not exhibit significant tendency, the distribution of median diameter along the coast will indicate that sands discharged from the Abukuma River and the Natori River are transported to the north. In Fig. 15—(b), the concentration of heavy minerals is high at the mouth of the Abukuma River and it decreases gradually to the north, but it decreases abruply to the south and increases again somewhat rapidly in the south area. Since the major source of the heavy minerals along the Sendai Coast is supposed to be the Abukuma River, the distribution of the concentration of heavy minerals shown in Fig. 15—(b) also indicates northward movement of sands discharged from the Abukuma River. Therefore, the high concentration of heavy minerals in the south area seems to have been originated in other sources.

The statistical analysis of the predominant direction of waves acting on the coast indicates the direction of sand drift clearly. Since the Kinka peninsula is pushing out into the sea at the northern end of the Sendai Coast, waves from the north are sheltered by the peninsula, whereas there is no obstacle to shelter waves from the south. Therefore, waves from the south which will cause sand

drift toward the north are predominant in the northern part of the Sendai Coast. Table 8 shows the result of statistical analysis of predominant wave direction observed at Gamou near the mouth of the Hichikita River 10 km north of the Natori River. In this table, the predominant wave direction is shown to be SSE as would be expected.

Table—8 Predominant Direction of Waves Observed at Gamou with Three Wave Meters (Obtained by the Shiogama Office of Second Harbour Construction Bureau in 1966)

Wave Direction	ESE	SE	SSE	S	Total
Number of Sample	0.7	81	260	79	423
Frequency (%)	3	19.1	61.5	18.7	100.0

As stated above, the results of analysis of sedimentary parameters, the concentration of heavy minerals in sands, and predominant wave direction have indicated that the predominant direction of sand drift along the coast at least north of the Abukuma River is to the northward. This indication is further strengthened by the distribution of foreshore slope along the coast. In general the finer the sands at foreshore is and the less the energy of waves acting on the coast is, the sharp the foreshore slope is. Figure 16 shows the distribution of foreshore slope along the Sendai Coast investigated by the Shiogama Office of Second

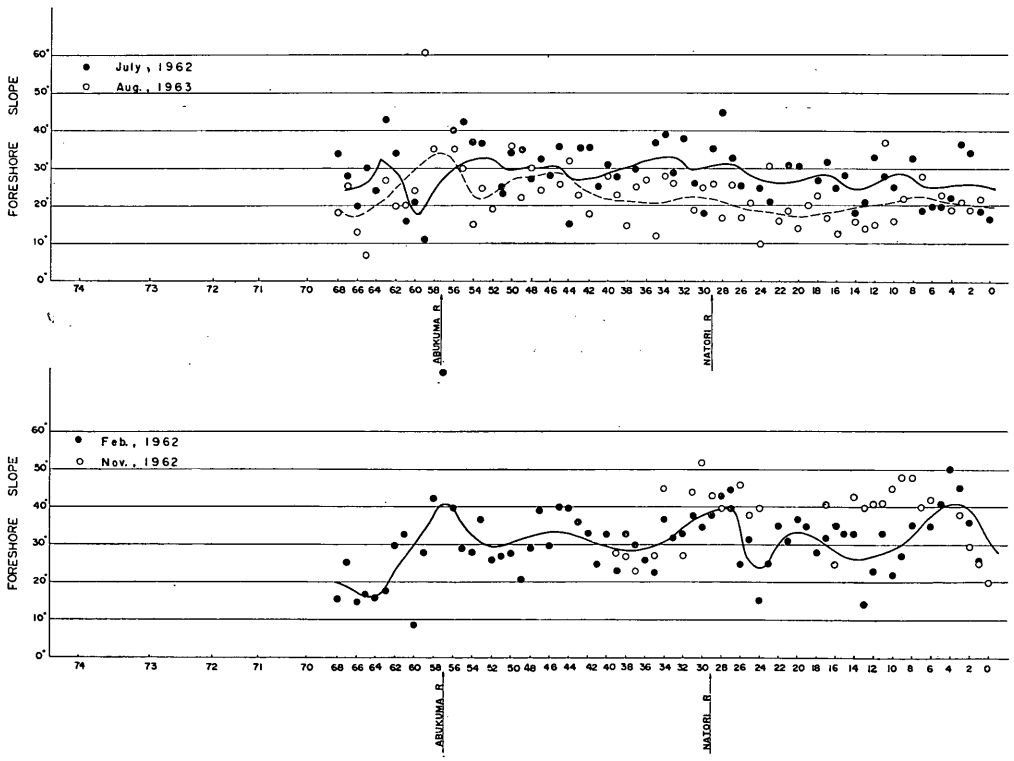

Fig. 16 Distribution of Foreshore Slope along the Sendai Coast

Harbour Construction Bureau in 1962 and 1963. The foreshore slope decreases from the Abukuma River to the north in summer, while it has no significant tendency in winter. In the coast facing the Paciffic Ocean, waves from the south due to typhoons act on the coast in summer and waves from the north due to depressions act on the coast in winter. The decrease of foreshore slope at the northern coast in summer in Fig. 16 cannot be the result of the increase of wave energy because there is no obstacle to shelter waves from the south in

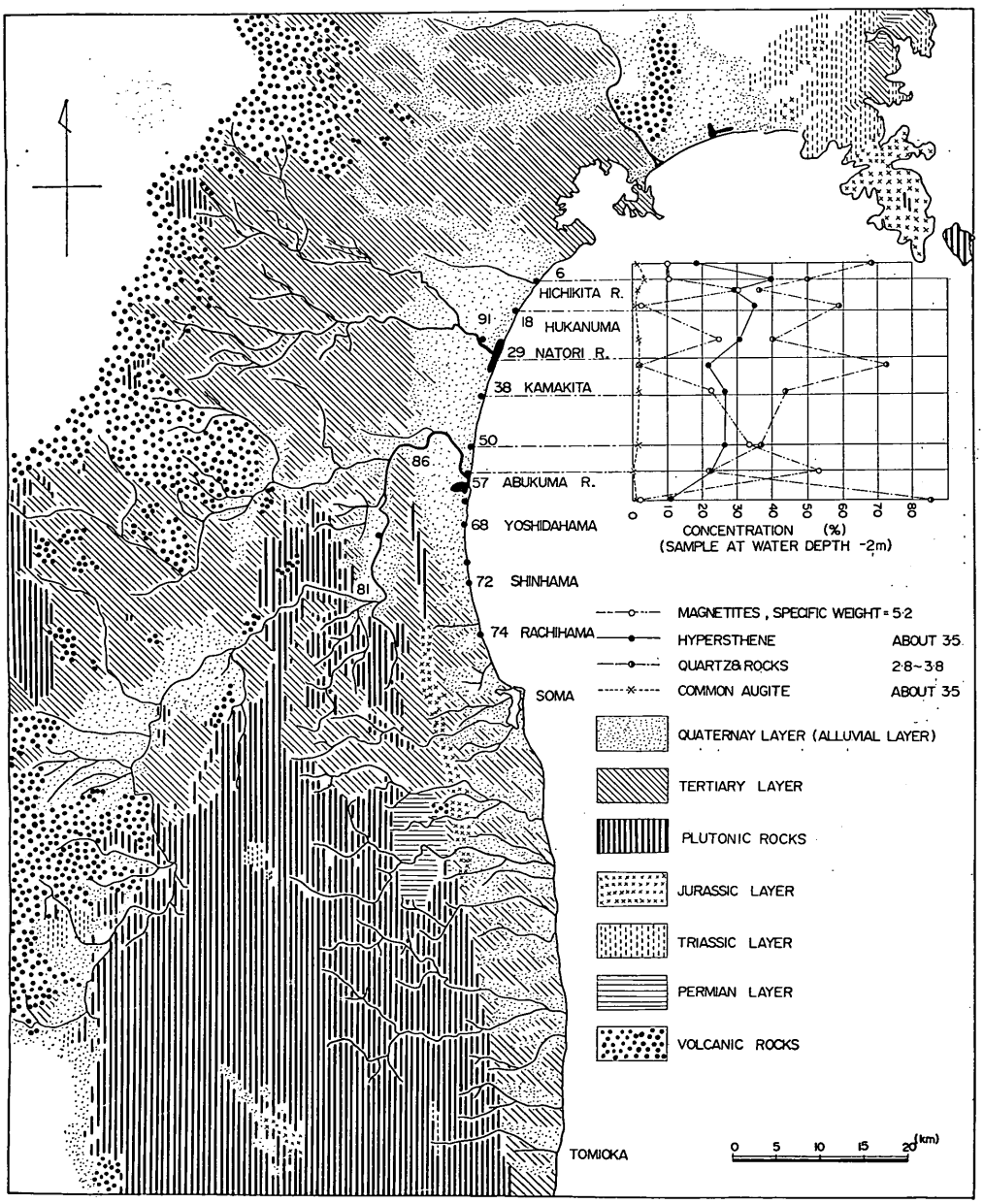

Fig. 17 Geological Map of Miyagi-Fukushima Prefecture

summer. Therefore, the decrease of foreshore slope at the northern coast must be due to the decrease of sand size at the northern coast. This sand size decrease will be attributed to the sorting of sands in which the finer sands are transported faster than the coarser sands in the direction of sand drift. On the other hand, since the distribution of foreshore slope has no significant tendency in winter, net movement of sand will not be remarkable during the season. The result of Fig. 16 indicates that the movement of sands to the north is strong in summer, but weak in winter.

5.2 Estimation of Sources and Direction of Sand Drift from the Data of Natural Vadioactive Tracers.

As shown in Table 2, thorium is concentrated in plutonic rocks such as diorite, granite rocks. Therefore, the geological map on the outcrop of the plutonic rocks will provide a reliable information on the sources of thorium supply to the coast. Figure 17 is a geological map of Miyagi-Fukushima prefecture. Plutonic rocks outcrop along the upper stream of the Abukuma River, while they are scarcely seen along the watershed of the Natori River. They also outcrop widely in the southern part of the Abukuma District and are very close to the coast from Soma to Tomioka. From these geological features, it is seen that the Abukuma River is the main source of thorium supply to the coast, and in addition, the rivers opening to the coast from Soma to Tomioka could also be the sources of thorium supply.

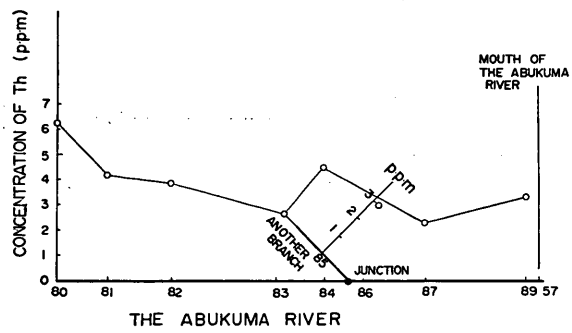

Fig. 18 Concentration of Thorium in Heavey Minerals along the Watershed of the Abukuma River

In order to confirm that the Abukuma River except the Natori River is the main source of thorium supply, the concentration of thorium in heavy minerals along the watershed of the Abukuma River and the Natori River was analyzed. The result of analysis of thorium concentration in heavy minerals along the Abukuma River has given the result shown in Fig. 18. The concentration of thorium is highest at the sampling point of No. 80, with the value of 6.3 p.p.m, which is just down-stream of the area where plutonic rocks outcrop. Although the content of thorium slightly decreases downstream, the concentration of thorium of nearly 3 to 4 p.p.m continues as far as the mouth of the Abukuma River. The concentration of thorium in heavy minerals along the watershed near the mouth of the Natori River is 1.6 p.p.m. From the results of the analysis of thorium in heavy minerals along rivers, it will be apparent that the Abukuma River is the main source of thorium supply to the Sendai Coast, and this estimation concides with that of the sources of thorium supply based on the geological map.

Now the sources of thorium supply being made clear, the next is the estimation of the direction of sand drift with natural radioactive tracers. The concentration of thorium in heavy minerals was calculated with Eq. (6) and the

concentration of thorium in sands including heavy minerals was obtained with the result of the calculation. Figures 19—(a) and (b) show the distribution of the concentration of thorium in sands and that in heavy minerals along the Sendai Coast respectively. Details of these are shown in Table 6 and 7. In Fig. 19—(a),

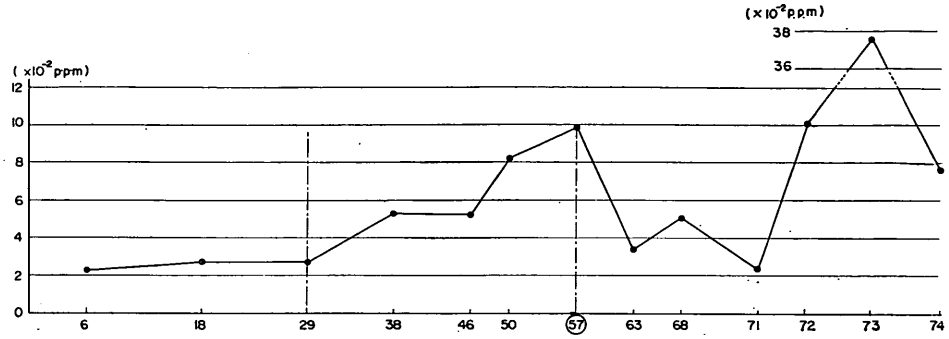

Fig. 19—(a) Distribution of the Concentration of Thorium in Sands along the Sendai Coast

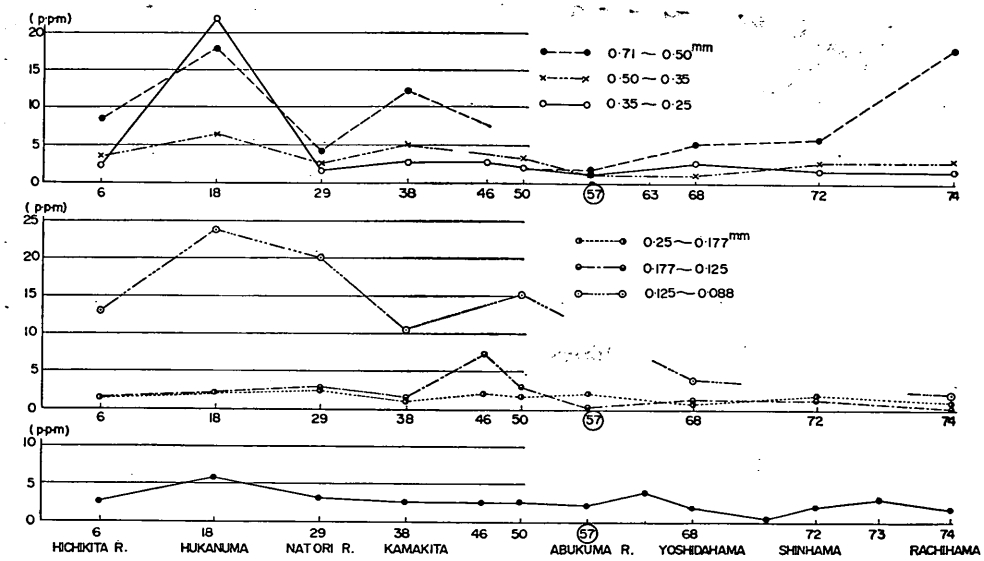

Fig. 19—(b) Distribution of the Concentration of Thorium in Heavy Minerals along the Sendai Coast

the concentration of thorium in sands is maximum at the mouth of the Abukuma River and decreases gradually to the north and becomes constant along the coast north of the Natori River. The concentration of thorium in sands decreases abruptly from the Abukuma River to the south and continues low concentration for a certain distance and increases again abruptly. In Fig. 19—(b), the concentration of thorium in heavy minerals of each size fraction seems to increase from the Abukuma River to the north. The average concentration of thorium in heavy minerals of total size fractions also shows the tendency to increase toward the north, although the tendency is not significant.

According to the results of analysis of sedimentary parameters, concentration of heavy minerals and predominant direction of waves, it is clear that the predominant direction of sand drift along the Sendai Coast is to the north. Since the Abukuma River is the main source of thorium supply to the coast, the distribution of the concentration of thorium in sands in Fig. 19—(a) seems to show that the majority of thorium discharged from the Abukuma River is supplied to the northern coast of the river and, therefore, the concentration of thorium in sands decreased in the direction of sand drift. The concentration of thorium in heavy minerals in Fig. 19—(b), however, showed the tendency to increase in the direction of sand drift. Kamel[1] estimated the direction of sand drift along the California Coast in the direction of decrease of the concentration of thorium in heavy minerals. Therefore, the result of analysis of the concentration of thorium in heavy minerals of the present study is contrary to Kamel's presumption. In order to interpret the increase of the concentration of thorium in heavy minerals in the direction of sand drift observed along the Sendai Coast, the sorting of sands by waves must be taken into consideration. Sands discharged from rivers undergo the action of waves and are transported in the direction of longshore current. In the course of the transportation, sands are sorted by waves and the heavier sands tend to remain behind the lighter sands. Therefore in natural beach, the concentration of the heavier sands will decrease in the direction of sand drift, and on the contrary, the concentration of lighter sands will increase in the same direction. These characteristics of the distribution of minerals are clearly seen in the result of mineralogical analysis of the Sendai Coast. The results of mineralogical analysis of beach sands made by Okitsu[5] are shown in Fig. 17. In this figure, the concentration of lighter minerals such as quartz, stone pieces, hypersthenite and augite increases to the north, namely to the direction of sand drift, while that of heavy minerals such as magnetic iron decreases to the same direction. The difference of these distributions with respect to the specific gravity of minerals is due to the sorting of minerals by waves. The concentration of thorium in heavy minerals seems to increase in the direction of sand drift because of this sorting of sands. In Table 2, the specific gravities of the most minerals rich in thorium content in the Abukuma District is less than the specific gravity of magnetic iron, which is the major component of heavy minerals along the Sendai Coast. As shown in Fig. 19—(b), the concentration of thorium in heavy minerals, therefore, increases in the direction of sand drift because minerals rich in thorium content are lighter than the average heavy minerals of this coast. Although Kamel (1962) estimated the predominant direction of sand drift on the presumption that the concentration of thorium in heavy minerals decreases in the direction of sand drift, if the minerals rich in thorium content are lighter than the average heavy minerals as in the case of the Sendai Coast, such presumption cannot be applied because of the sorting of sands by waves.

Since the variation of the distribution of natural tracers along the coast is the result of the sorting of sands by waves, the concentration of thorium in sands would indicate the direction of sand drift more clearly than that in heavy minerals because of the greater difference of specific gravity between the minerals rich in thorium content and sands than that between the minerals rich in thorium content and heavy minerals. Therefore, it will be preferable to use the index of the concentration of thorium in sands instead of that in heavy minerals

Table—4 Sedimentary Paramenters

Sample	Median diameter			Sorting coefficient	Skewness
No.	d_{50}	d_{75}	d_{25}	$(d_{75}/d_{25})^{1/2}$	$d_{25} \times d_{75}/d_{50}$
2	0.28	0.36	0.24	1.225	0.3085
4	0.50	0.60	0.42	1.195	0.5040
6	0.42	0.52	0.34	1.235	0.4209
9	0.42	0.54	0.36	1.225	0.4628
13	0.41	0.53	0.31	1.305	0.4007
18	0.41	0.56	0.295	1.375	0.4029
22	0.33	0.46	0.25	1.385	0.3636
25	0.56	0.74	0.38	1.395	0.5021
28	0.51	0.40	0.39	1.012	0.3058
29	0.69	0.94	0.34	1.66	0.4631
32	0.30	0.41	0.24	1.305	0.3280
35	0.39	0.62	0.28	1.485	0.4451
38	0.31	0.44	0.24	1.68	0.3406
42	0.42	0.58	0.30	1.39	0.4142
46	0.35	0.48	0.245	1.4	0.3360
50	0.55	0.72	0.38	1.356	0.4974
53	0.63	0.82	0.49	1.276	0.6222
55	0.55	0.76	0.42	1.345	0.5803
55	0.43	0.48	0.38	1.112	0.4241
57	0.85	1.35	0.59	1.51	0.937
59	0.40	0.54	0.29	1.363	0.3915
60	0.38	0.46	0.29	1.257	0.351
61	0.30	0.38	0.25	1.232	0.3166
63	0.41	0.46	0.365	1.122	0.4095
65	0.32	0.415	0.25	1.42	0.3242
68	0.39	0.45	0.34	1.15	0.3923
71	0.49	1.05	0.40	1.625	0.8571
72	0.39	0.53	0.28	1.375	0.3805
73	0.35	0.43	0.25	1.305	0.3071
74	0.28	0.36	0.21	1.305	0.2700
80	0.64	0.85	0.42	1.43	0.5643
81	0.40	0.53	0.305	1.32	0.4041
82	0.52	0.63	0.42	1.225	0.5088
83	0.41	0.46	0.35	1.145	0.3926
84	0.13	0.19	0.075	1.59	0.1096
85	0.61	1.4	0.32	2.09	0.7344
86	0.87	2.4	0.54	2.105	1.489
87	0.44	0.58	0.30	1.39	0.3954
89	0.57	0.98	0.52	1.37	0.894
91	0.17	0.48	0.078	2.48	0.2202
93	0.22	0.49	0.1	2.215	0.2227

Table—5 Concentration of Heavy Minerals in Sands

Sample No.	Location	Size fraction analyzed	Weight of total sample in size fraction (gr)	Weight of heavies in size fraction (gr)	Concentration of heavies in sand (%)	Mean concentration of heavies in sand (%)
No. 2		3	88.29			
		4	270.15			
		5	468.53			
		6	438.51	1.96	0.45	
		7	33.47	2.44	7.31	
		8	9.00	0.40	4.45	
		(Total)	1319.30	4.80		0.36
No. 4		2	114.81	0.07	0.06	
		3	605.90	0.33	0.05	
		4	652.40	0.69	0.11	
		5	45.31	0.04	0.09	
		6	48.84	1.21	2.48	
		7	3.66	1.17	31.91	
		8	0	0	0	
		9	1.36	0.18	13.24	
		(Total)	1472.28	3.69		0.25
No. 6	Hichikita R.	3	14.24	0	0	
		4	466.70	0.69	0.15	
		5	910.80	2.89	0.32	
		6	246.20	2.06	0.84	
		7	113.50	6.02	5.31	
		8	6.83	2.55	37.79	
		9	0.28	0.15	54.29	
		10	0.99	0.42	41.92	
		(Total)	1759.54	14.78		0.84
No. 9		2	76.87			
		3	583.09			
		4	965.07			
		5	297.37	3.29	2.20	
		6	149.63	1.96	29.70	
		7	6.61			
		8	0			
		9	1.83			
		(Total)	2080.47	5.25		0.25
No. 13		2	76.68			
		3	531.84			
		4	647.81			
		5	558.52			

Sample No.	Location	Size fraction analyzed	Weight of total sample in size fraction (gr)	Weight of heavies in size fraction (gr)	Concentration of heavies in sand (%)	Mean concentration of heavies in sand (%)
		6	115.38	4.94	4.28	
		7	8.00	1.94	24.28	
		8	0			
		9	3.12			
		(Total)	1941.35	6.88		0.35
No. 18	Hukanuma	2	144.13	0.11	0.08	
		3	668.77	0.68	0.10	
		4	588.91	0.80	0.14	
		5	625.38	0.20	0.03	
		6	347.15	6.42	1.85	
		7	24.27	0	0	
		8	0.94	0.26	27.12	
		9	3.82	0.27	7.16	
		(Total)	2403.37	8.74		0.36
No. 22		2	101.51			
		3	271.80			
		4	367.46			
		5	472.38			
		6	374.66	16.53	4.41	
		7	36.97	11.04	29.86	
		8	1.70	0.50	29.62	
		9	4.92			
		(Total)	1631.40	28.07		1.72
No. 25		2	509.54			
		3	561.31			
		4	404.74			
		5	303.57	6.31	0.33	
		6	113.34	4.04	0.21	
		7	8.36	0.26	0.01	
		8	0.61	0		
		9	0.79			
No. 28		(Total)	1902.26	10.61		0.56
		2	56.70			
		3	301.15			
		4	224.39			
		5	59.43			
		6	16.18	6.81	42.21	
		7	2.73	0.59	80.98	
		8	0	0		

Sample No.	Location	Size fraction analyzed	Weight of total sample in size fraction (gr)	Weight of heavies in size fraction (gr)	Concentration of heavies in sand (%)	Mean concentration of heavies in sand (%)
		9	0.63			
		(Total)	559.21			1.12
No. 29		2	956.87	0.60	0.10	
		3	678.43	2.17	0.30	
		4	282.50	3.64	1.29	
		5	72.52	4.52	5.91	
		6	7.54	2.71	30.30	
		7	8.00	3.24	40.53	
		8	0.69	0.18	25.54	
		9	1.81	0	0	
		10		0.05	2.68	
		(Total)	2008.36	17.28		
No. 32		2	52.26	0.10	0.19	
		3	189.19	0.50	0.26	
		4	1009.20	12.67	1.26	
		5	283.00	3.73	1.32	
		6	237.00	18.33	7.74	
		7	16.22	9.05	55.79	
		8	0.51	0		
		9	3.75			
		(Total)	1791.13	44.38		2.48
No. 35		2	181.13	0.22	0.12	
		3	180.50	0.66	0.37	
		4	230.50	1.07	0.74	
		5	274.50	1.32	0.48	
		6	142.50	6.90	4.84	
		7	7.97	2.62	32.85	
		8	1.15	0.36	30.96	
		9	6.73	1.18	30.39	
		10		1.24	43.37	
		(Total)	1024.98	15.57		1.52
No. 38	Kamakita	2	84.09	0	0	
		3	206.60	0.76	0.37	
		4	347.25	1.56	0.45	
		5	535.10	3.30	0.62	
		6	448.58	13.12	3.04	
		7	51.21	11.87	23.17	
		8	1.41	0.86	60.68	
		9	1.74	0.21	71.24	

Sample No.	Location	Size fraction analyzed	Weight of total sample in size fraction (gr)	Weight of heavies in size fraction (gr)	Concentration of heavies in sand (%)	Mean concentration of heavies in sand (%)
		10		0.53	36.87	
		(Total)	1675.98	32.71		1.95
No. 42		2	214.67			
		3	355.03			
		4	434.67			
		5	415.32			
		6	156.33	20.13	12.80	
		7	10.39	6.37	61.29	
		8	0.81	0.20	24.82	
		9	1.69			
		(Total)	1588.91	26.70		1.68
No. 46		2	51.01			
		3	313.95			
		4	545.20			
		5	475.04	21.53	4.53	
		6	468.47	11.66	2.49	
		7	68.13	1.68	2.46	
		8	2.70			
		9	1.66			
		(Total)	1926.16	34.87		1.81
No. 50		2	478.72	0.43	0.19	
		3	548.00	9.86	1.80	
		4	436.10	1.74	0.40	
		5	214.50	12.18	5.68	
		6	123.50	24.57	19.90	
		7	12.12	7.29	60.12	
		8	0.78	0.52	66.28	
		9	1.12			
		(Total)	1814.83	56.59		3.12
No. 53		2	957.71	11.71		
		3	1131.70			
		4	598.70	120.25	20.08	
		5	135.50	71.10	52.50	
		6	47.22	33.15	70.20	
		7	8.22	7.35	89.38	
		8				
		9	2.92			
		(Total)	2881.97	243.56		8.45

Sample No.	Location	Size fraction analyzed	Weight of total sample in size fraction (gr)	Weight of heavies in size fraction (gr)	Concentration of heavies in sand (%)	Mean concentration of heavies in sand (%)
No. 55		2	314.55			
		3	403.11			
		4	729.57			
		5	695.08			
		6	216.41			
		7	105.85	39.99	37.78	
		8	9.03	6.03	66.74	
		9	0.71	0.39	53.92	
		10	1.89			
		(Total)	2476.30	46.41		1.80
No. 57	Abukuma R.	1	941.89	1.83	0.19	
		2	293.32	5.38	1.83	
		3	724.44	30.42	4.20	
		4	220.42	36.53	16.57	
		5	56.39	22.15	39.28	
		6	11.33	6.10	53.82	
		7	1.57	0.70	44.96	
		8				
		9				
		10	2.45			
		(Total)	2251.81	103.11		4.58
No. 59		1	205.26			
		2	150.23			
		3	191.21			
		4	845.76			
		5	268.11	7.16	2.67	
		6	374.83	27.06	7.22	
		7	39.96	10.80	27.03	
		8	2.84	1.96	69.16	
		9	0.96			
		10	4.11			
		(Total)	2083.27	46.98		2.26
No. 60		1	21.08	0		
		2	38.70	0		
		3	129.00	0.44	0.34	
		4	735.40	5.50	0.75	
		5	365.50	2.61	0.71	
		6	161.40	14.67	9.09	
		7	78.97	17.27	21.80	
		8	3.45	2.78	80.04	

Sample No.	Location	Size fraction analyzed	Weight of total sample in size fraction (gr)	Weight of heavies in size fraction (gr)	Concentration of heavies in sand (%)	Mean concentration of heavies in sand (%)
		9	0	0	0	
		10	10.15	6.18	60.90	
		(Total)	1543.65	49.45		3.20
No. 61		2	0.88	0		
		3	61.24	0.19	0.31	
		4	360.50	0.48	0.13	
		5	576.70	2.15	0.37	
		6	329.20	7.80	2.37	
		7	38.53	10.20	26.47	
		8	3.32	2.56	77.16	
		9	0.11	0.05	43.36	
		10	0.94	0		
		(Total)	1371.42	23.43		1.71
No. 63		2	8.95			
		3	140.50	0.54	0.38	
		4	1286.10	1.86	0.14	
		5	237.50	0.41	0.17	
		6	29.70	7.05	23.72	
		7	1.86	1.41	75.70	
		8	1.05	0.66	63.54	
		9	0.58			
		10	1.08			
		(Total)	1707.32	11.93		0.70
No. 65		2	1.09			
		3	61.41			
		4	734.34	0.55	0.07	
		5	416.14	0.30	0.07	
		6	576.81	8.85	1.54	
		7	55.66	7.14	12.82	
		8	3.63	2.15	59.16	
		9	1.28			
		10	0.78			
		(Total)	1851.07	18.19		1.03
No. 68	Yoshidahama	2	1.50	0.03		
		3	105.80	2.35	2.22	
		4	1122.80	14.30	1.27	
		5	262.32	2.77	1.06	
		6	193.22	18.57	9.61	
		7	19.07	6.68	35.02	
		8	1.92	1.61	83.64	

Sample No.	Location	Size fraction analyzed	Weight of total sample in size fraction (gr)	Weight of heavies in size fraction (gr)	Concentration of heavies in sand (%)	Mean concentration of heavies in sand (%)
		9	0	0		
		10	1.54	0.97		
		(Total)	1708.17	47.27		2.77
No. 71		1	357.68			
		2	71.00			
		3	120.00	0.12	0.10	
		4	517.50	9.56	1.89	
		5	29.61			
		6	86.50	12.20	14.10	
		7	19.62	8.90	45.38	
		(Total)	1201.91	30.78		2.56
No. 72		1	5.61	0.02	0.41	
		2	40.95	0		
		3	231.70	1.29	0.56	
		4	298.70	5.38	1.81	
		5	257.50	8.07	3.13	
		6	145.50	19.26	13.24	
		7	27.47	19.47	70.86	
		(Total)	1007.43	53.49		5.31
No. 73		1	21.21	0	0	
		2	32.01	0	0	
		3	180.70	3.18	1.76	
		4	860.70	48.51	5.64	
		5	616.20	44.09	7.15	
		6	448.70	122.19	27.23	
		7	71.75	43.00	59.92	
		8	0.71	0		
		9	0	0		
		10	39.43	8.24	20.90	
		(Total)	2271.41	269.21		
No. 74		2	1.18	0		
		3	37.04	0.50	1.36	
		4	489.15	5.98	1.22	
		5	581.92	6.51	1.12	
		6	651.74	28.64	4.40	
		7	102.17	28.48	27.88	
		8	14.56	8.26	56.75	
		9	0			
		10	4.01	1.77	44.04	
		(Total)	1881.77	80.14		4.26

Table—6 Concentration of Thorium in Heavy Minerals of Each Size Fraction

Sample No.	Size fraction analyzed	Counting rate of photo-peak c	Weight of sample w (gr)	c/w	Concentration of thorium (p.p.m)
No. 6	2				
	3	57.7	0.689	83.8	8.4
	4	101.5	2.879	35.3	3.5
	5	45.2	2.023	22.3	2.2
	6	86.8	5.983	14.5	1.5
	7	38.0	2.530	15.0	1.5
	8	20.5	0.159	12.9	1.3
	9+10	53.0	0.400	13.2	1.3
No. 18	2	87.0	0.103	837	83.7
	3	103.0	0.576	179	17.9
	4	50.6	0.778	65	6.5
	5	41.4	0.190	218	21.8
	6	13.0	6.331	41.2	2.1
	7	0	0	0	0
	8	57.0	0.239	238	23.8
	10		0.241		14.9
No. 29	1	34.6	0.154	22.5	2.25
	2	45.6	0.605	75.4	7.5
	3	88.0	2.173	40.5	4.1
	4	93.8	3.641	25.7	2.6
	5	70.0	4.512	15.5	1.6
	6	71.0	2.700	26.3	2.6
	7	93.5	3.237	28.9	2.9
	8	35.0	0.174	20.1	2.0
No. 38	3	68.0	0.557	122	12.2
	4	80.9	1.550	52.2	5.2
	5	87.2	3.290	26.5	2.7
	6	80.3	7.975	10.1	1.0
	7	161.1	9.053	17.8	1.8
	8	90.6	0.854	106	10.6
	9	82.0	0.730	112	11.2
No. 46	5	152	5.326	28.5	2.85
	6	218	9.913	22.0	2.20
	7	102	1.398	73.0	7.30
No. 50	2	141.0	0.423	333	33.3
	3	164.0	9.064	18.1	1.8
	4	59.0	1.725	34.3	3.4

Sample No.	Size fraction analyzed	Counting rate of photo-peak c	Weight of sample w (gr)	c/w	Concentration of thorium (p.p.m)
	5	170.1	8.705	19.5	2.0
	6	143.0	9.688	14.8	1.5
	7	226.0	7.220	31.3	3.1
	8	77.8	0.510	15.3	1.5
No. 57	2	242.0	1.820	133	13.3
	3	155.0	8.293	18.7	1.9
	4	97.0	8.660	11.2	1.1
	5	103.0	8.185	12.6	1.2
	6	133.0	6.089	21.8	2.2
	7	3.0	0.699	4.3	0.4
No. 68	3	125	2.348	53.2	5.3
	4	140	10.384	13.5	1.3
	5	78.1	2.758	28.3	2.8
	6	97.9	10.724	9.1	0.9
	7	94	6.636	14.2	1.4
	8	63	1.559	40.4	4.0
	10	67.2	0.959	70.0	7.0
No. 72	3	116	1.94	59.8	6.0
	4	153	5.35	28.6	2.9
	5	142	8.035	17.7	1.8
	6	133	7.008	19.0	1.9
	7	117.7	9.102	12.9	1.3
No. 74	3	90.2	0.502	18.0	1.8
	4	182	5.97	30.5	3.1
	5	113	6.51	17.4	1.7
	6	100.1	10.562	10.0	1.0
	7	21	10.056	2.1	0.2
	8	165.8	8.212	20.2	2.0
	10	115	1.735	66.3	6.6

Cf. In Table 6, Figures of the Size Fraction in the Column 2 denotes;

1 above 1.0 mm	2 0.71~1.0 mm	3 0.5~0.71 mm
4 0.35~0.5 mm	5 0.25~0.35 mm	6 0.177~0.25 mm
7 0.125~0.177 mm	8 0.088~0.125 mm	9 below 0.088 mm

Table—7 Concentration of Thorium in Heavy Minerals and Sands

Sample No.	Location	Concentration of thorium in heavies (p.p.m)	Concentration of thorium in sand (p.p.m)
6	Hichikita R.	2.64	2.21×10^{-2}
29	Natori R.	2.27	2.38
38	Kamakita	2.97	5.79
46		2.84	5.20
50		2.25	7.01
57	Abukuma R.	2.05	9.39
63		4.80	3.35
68	Yoshidahama	1.79	4.95
71		0.66	1.68
72	Shinhama	1.87	9.93
73		3.17	37.60
74	Rachihama	1.73	7.28

in order to estimate sources and direction of sand drift. The estimation of sources and predominant direction of sand drift in the case of the Sendai Coast with the index of the concentration of thorium in sands in Fig. 19—(a) is be as follows:

According to the geological map in Fig. 17, the main sources of thorium supply to the coast are the Abukuma River and the rivers opening to the coast from Soma to Tomioka. From the distribution of the concentration of thorium in sands in Fig. 19—(a), the supply of sands discharged from the Abukuma River is limitted several kilometers to the south and most of sands discharged from the Abukuma River is transported to the north. Although this supply of sands from the Abukuma River is predominant as far as the Natori River, beach sands north of the Natori River are supplied mainly by the Natori River because the concentration of thorium along the coast north of the Natori River is as low as the background and changes very little along the coast. The high concentration of thorium in sands at the southern coast from No. 71 to 74 will originate in the rivers opening to the coast from Soma to Tomioka because thorium discharged from the Abukuma River are transported to the north and, therefore, there is no source of thorium supply except these rivers. Consequently, the predominant direction of sand drift along the Sendai Coast is northward except the coast for several kilometers south from the Abukuma River.

9. Conclusions

The use of natural radioactive tracers for the estimation of sources and direction of sand drift was examined in the case of the Sendai Coast on the presumption that the predominant direction of sand drift along the coast north of the Abukuma River is northward.

The conclusions of the present study are as follows:

(1) The sources of thorium supply in the coast like the Sendai Coast which has somewhat simple geological features can be estimated with the geological

map which shows the geological features on the outcrop of plutonic rocks.

(2) The concentration of thorium in heavy minerals increases in the direction of sand drift along the coast like the Sendai Coast where minerals rich in thorium content are lighter than the average heavy minerals.

(3) The concentration of thorium in sands decreases in the direction of sand drift. This will indicate the direction of sand drift more clearly than that in heavy minerals because the specific gravity of the minerals rich in thorium content is always larger than that of sands but may be smaller than that of some heavy minerals.

It should be noted that in estimating the sources of thorium supply, the employment of only geological maps is enough for the case in which geological features are simple like the Sendai Coast. In the case that geological features are complicated, the detailed sampling accompanied by the detailed geological maps will be necessary for the estimation of sources and direction of sand drift with natural radioactive tracers.

Acknowledgements

The authors wish to express their appreciation to Mr. Norio Tanaka, senior research engineer of Hydraulics Division of Port and Harbour Research Institute for his helpful suggestion and Messers. Shigenobu Sugiyama and Takeshi Horie who performed investigational work and helped in arranging the data of investigation.

References

1) Adel M. Kamel: "Littoral Studies Near San Fransisco Using Tracer Techniques," Technical Memorandum No. 131, Beach Erosion Board, Nov. 1962.
2) "Geological Handbook," editted by Haruyoshi Fujimoto et al, Asakura-Shoten Press Company, 1966. (in Japanese)
3) "Uranium," editted by The Research Committee of Uranium and Thorium, Asakura-Shoten Press Company, 1967. (in Japanese)
4) Adams, John A. S., et al, "Determination of Thorium and Uranium in Sedimentary Rocks by Two Independent Methods," Geochemica. et. Cosmo Chemica Acta, Vol. 13, 1958.
5) "The Geological Map of Miyagi District," published by the Department of Science of Tohoku University, 1962. (in Japanese)